Internal Jet Structure in Dijet Production in Deep-Inelastic Scattering

Peer-Oliver Meyer[a] for the H1 Collaboration

[a]III. Physikalisches Institut, RWTH Aachen, D-52056 Aachen, Germany

The internal jet structure in dijet production in deep-inelastic scattering is measured with the H1 detector at HERA. Jets with transverse energies $E_{T,\mathrm{Breit}} > 5\,\mathrm{GeV}$ are selected in the Breit frame employing $k_\perp$ and cone jet algorithms in the kinematic region of squared momentum transfers of $10 < Q^2 \lesssim 120\,\mathrm{GeV}^2$ and x-Bjorken values of $2 \cdot 10^{-4} \lesssim x_{\mathrm{Bj}} \lesssim 8 \cdot 10^{-3}$. Jet shapes and subjet multiplicities are measured as functions of a resolution parameter. The corrected data are well described by QCD models. It is observed that jets are more collimated with increasing transverse jet energies and decreasing pseudo-rapidities, i.e. towards the photon direction. Comparisons with OPAL data show that jet shapes of jets measured in $\gamma\gamma$ collisions are very similar to those measured in ep collisions.

1. INTRODUCTION

The internal structure of jets is sensitive to the mechanism by which a complex aggregate of observable hadrons evolves from a hard process. It is expected that the internal structure of jets depends mainly on the type of the primary parton, quark or gluon, from which it originated and to a lesser extent on the particular hard scattering process. Measurements of the internal structure of jets have been made in $p\bar{p}$ collisions and in e^+e^- annihilations. At the $e^\pm p$ collider HERA jet shapes have been investigated in photoproduction ($Q^2 \approx 0\,\mathrm{GeV}^2$) [1] and in deep-inelastic scattering at $Q^2 > 100\,\mathrm{GeV}^2$ [2].

Here we present the measurements of internal jet structure [3] in a sample of inclusive dijet events with transverse jet energies of $E_{T,\mathrm{Breit}} > 5\,\mathrm{GeV}$ in the kinematic range of $10 < Q^2 \lesssim 120\ \mathrm{GeV}^2$ and $2 \cdot 10^{-4} \lesssim x_{\mathrm{Bj}} \lesssim 8 \cdot 10^{-3}$. Jets are defined in the Breit frame by the $k_\perp$ [4] and the cone [5] jet algorithm. The analysis is based on data taken in 1994 with the H1 detector at HERA, operated with positrons of energy $E_e = 27.5\,\mathrm{GeV}$ colliding with protons of energy $E_p = 820\,\mathrm{GeV}$. The data correspond to an integrated luminosity of $\mathcal{L}_{\mathrm{int}} \simeq 2\,\mathrm{pb}^{-1}$. Two observables, jet shapes and subjet multiplicities, are studied. Both observables are corrected for detector effects and are presented as a function of the transverse jet energy and the jet pseudo-rapidity.

2. OBSERVABLES

The jet shape $\Psi(r)$ is defined as the average fractional transverse jet energy that lies in a subcone of radius r concentric with the jet axis

$$\Psi(r) \equiv \frac{1}{N_{\mathrm{jets}}} \sum_{\mathrm{jets}} \frac{E_T(r)}{E_{T,\mathrm{jet}}}\,. \qquad (1)$$

N_{jets} is the total number of jets in the sample and $E_T(r)$ is the transverse energy within a subcone of radius r. A natural variable for studying the internal structure of jets with the $k_\perp$ cluster algorithm is the multiplicity of subjets, resolved at a resolution scale which is a fraction of the jet's transverse energy. For each jet in the sample the clustering procedure is repeated for all particles assigned to the jet. The clustering is stopped when the distances y_{ij} between all particles i, j are above some cut-off y_{cut}

$$y_{ij} = \frac{\min(E_{T,i}^2, E_{T,j}^2)}{E_{T,\mathrm{jet}}^2} \frac{(\Delta\eta_{ij}^2 + \Delta\phi_{ij}^2)}{R_0^2} > y_{\mathrm{cut}} \qquad (2)$$

where R_0 is set to $R_0 = 1.0$. The remaining (pseudo-)particles are called subjets. The parameter y_{cut} defines the minimal relative transverse energy between subjets inside the jet and thus determines the extent to which the internal jet structure is resolved.

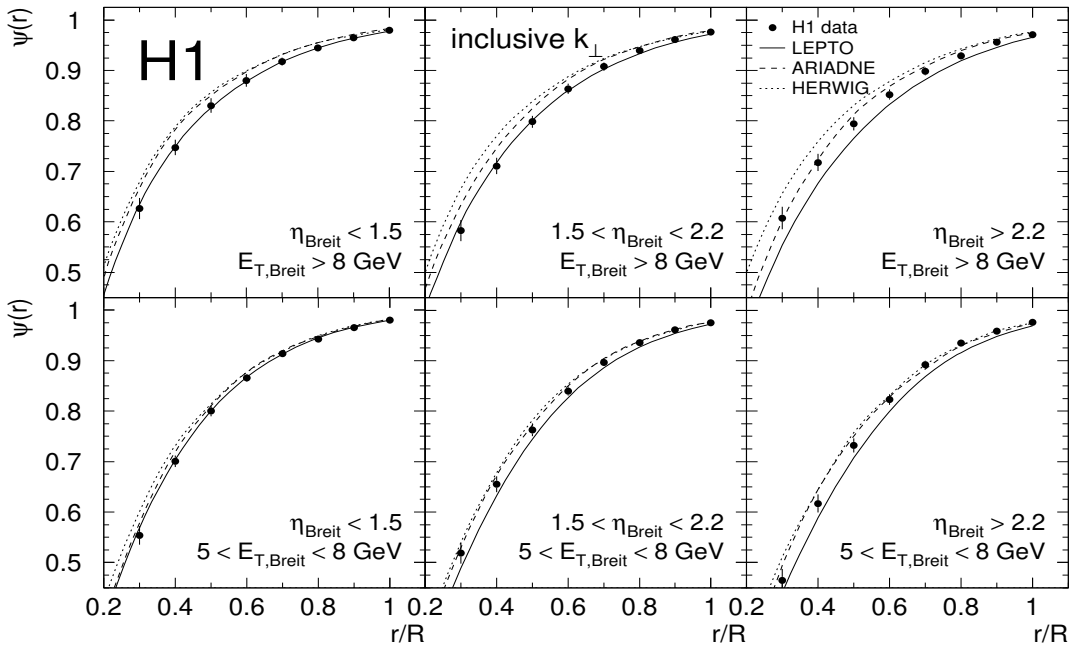

Figure 1. The jet shapes for the inclusive $k_\perp$ algorithm. The data are shown as a function of the transverse jet energy and the jet pseudo-rapidity in the Breit frame (positive pseudo-rapidities are towards the proton direction). The results are compared to predictions of QCD models.

3. RESULTS

The radial dependence of the jet shape $\Psi(r)$ for the $k_\perp$ algorithm is shown in Fig. 1 in different ranges of the pseudo-rapidity and transverse jet energy in the Breit frame. The predictions of three QCD models are overlaid. The jet shape $\Psi(r)$ increases faster with r for jets at larger E_T, indicating that these jets are more collimated. Jets towards the proton direction (at larger values of $\eta_{\rm Breit}$) are broader than jets towards the photon direction (smaller $\eta_{\rm Breit}$).

The QCD models LEPTO, ARIADNE and HERWIG all show $E_{T,\rm Breit}$ and $\eta_{\rm Breit}$ dependencies similar to those seen in the data. LEPTO gives a good overall description of the data although it has the tendency to produce broader jets in the proton direction. A good description is also obtained by the ARIADNE model except for jets at smaller pseudo-rapidities where the jet shapes have the tendency of being too narrow. For the HERWIG model the jet shapes are slightly narrower than those in the data in all $E_{T,\rm Breit}$ and $\eta_{\rm Breit}$ regions.

Fig. 2 shows the jet shapes and the subjet multiplicities for the $k_\perp$ algorithm as predicted by the LEPTO parton shower model, separately for quark and gluon jets at $E_{T,\rm Breit} > 8\,\rm GeV$ and $\eta_{\rm Breit} < 1.5$. Within this model gluon jets are broader than quark jets. The same prediction is obtained by the HERWIG parton shower model. In the phase space considered here, LEPTO and HERWIG (in agreement with next-to-leading order calculations) predict a fraction of approx. 80 % photon-gluon fusion events with two quarks in the partonic final state. The jet samples of these models are therefore dominated by quark jets. Both model predictions for the jet shapes and the subjet multiplicities therefore mainly reflect the properties of the quark jets as can be seen in Fig. 2. These predictions give a good description of the data. Thus, we conclude, that the jets we observe are consistent with being mainly initiated by quarks.

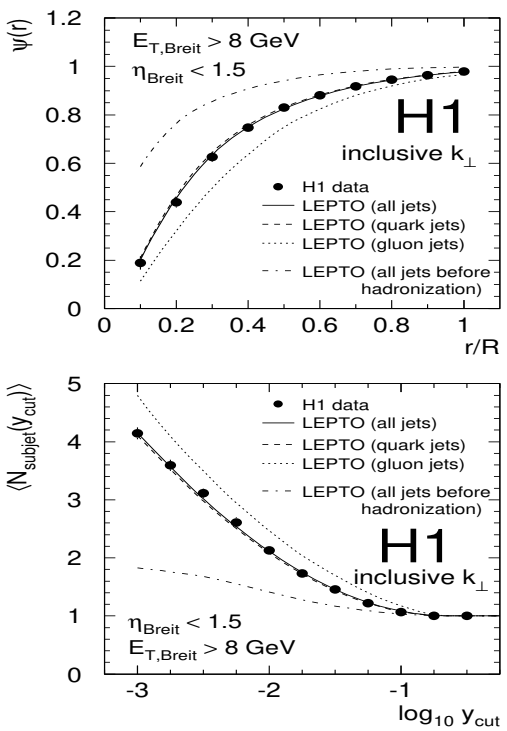

Figure 2. Model predictions of the internal structure of quark and gluon jets for the inclusive $k_\perp$ algorithm by the LEPTO parton shower model. The jet shapes (top) and the subjet multiplicities (bottom) are shown separately for quark and gluon induced jets with $E_{T,\mathrm{Breit}} > 8\,\mathrm{GeV}$ and $\eta_{\mathrm{Breit}} < 1.5$, together with the sum of both and the comparison to the H1 measurement. The distributions of the observables before hadronization are also shown.

Fig. 3 shows the jet shapes for the cone algorithm in the backward region ($\eta_{\mathrm{Breit}} < 1.5$) for two regions of $E_{T,\mathrm{Breit}}$. As seen for the $k_\perp$ algorithm in Fig. 1 jets with larger transverse energy $E_{T,\mathrm{Breit}}$ are more collimated.

The results are compared to the jet shapes measured by OPAL in $\gamma\gamma$ collisions [6] in similar E_T regions. Although these jets are produced in a different scattering process, their jet shapes are very similar to those measured in ep collisions. This indicates that the internal jet structure does not depend on the underlying hard process.

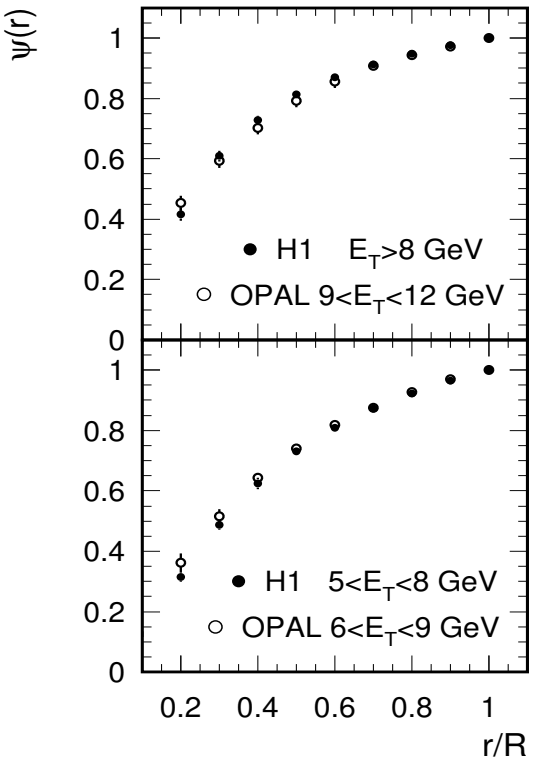

Figure 3. Jet shapes for the cone algorithm at $\eta_{\mathrm{Breit}} < 1.5$. The jet shapes of jets measured by OPAL in $\gamma\gamma$ collisions are overlaid. The comparison is shown for two different regions of transverse jet energies.

REFERENCES

1. ZEUS Collaboration, J. Breitweg et al., Eur. Phys. J. **C2** (1998) 61.
2. ZEUS Collaboration, J. Breitweg et al., DESY 98-038, Hamburg, Germany (1998)
3. H1 Collaboration, C. Adloff et al., Nucl. Phys. **B545** (1999) 3.
4. S.D. Ellis, D.E. Soper, Phys. Rev. **D48** (1993) 3160.
5. L.A. del Pozo, PhD Thesis University of Cambridge, Cambridge, England (1993) RALT-002
6. OPAL Collaboration, G. Abbiendi et al., CERN-EP/98-113.